Supplement

Development of the global chemistry-climate coupled model BCC-GEOS-Chem v2.0: improved atmospheric chemistry performance and new capability of chemistry-climate interactions

Ruize Sun[1#], Xiao Lu[2#], Haipeng Lin[3], Tongwen Wu[4], Xingpei Ye[1], Lu Shen[1], Xuan Wang[5], Haolin Wang[2], Jingyu Li[2], Ni Lu[1], Jiayin Su[2], Jie Zhang[4], Fang Zhang[4], Xiaoge Xin[4], Xiong Liu[6], Lin Zhang[1]

[1]Department of Atmospheric and Oceanic Sciences, School of Physics, Peking University, Beijing, China
[2]School of Atmospheric Sciences, Sun Yat-sen University, Zhuhai, Guangdong, China
[3]John A. Paulson School of Engineering and Applied Sciences, Harvard University, Cambridge, MA, United States of America
[4]Beijing Climate Center, China Meteorological Administration, Beijing, China
[5]School of Energy and Environment, City University of Hong Kong, Hong Kong SAR, China
[6]Harvard–Smithsonian Center for Astrophysics, Cambridge, MA 02138, USA

 # These authors contributed equally to this work.

Correspondence to: Lin Zhang (zhanglg@pku.edu.cn)

Table S1. Comparison of global annual emissions in BCC-GEOS-Chem v2.0

Main species	BCC-GEOS-Chem v2.0	BCC-GEOS-Chem v1.0	BCC-AGCM-Chem	Classic GEOS-Chem [a]
NO [b]	118.1	111.1	110.3	113.6
CO	926.2	925.5	1140.6	925.9
ISOP	389.4	410.0	410.8	367.2
Other species	**BCC-GEOS-Chem v2.0**	**BCC-GEOS-Chem v1.0**	**BCC-AGCM-Chem**	**Classic GEOS-Chem**
ALK4	54.7	44.0	\	52.9
BC	8.0	9.2	9.2	8.0
BENZ	7.8	6.7	\	7.8
C2H6	13.2	9.3	\	14.4
C3H8	14.5	7.2	\	14.4
CH2O	6.5	5.7	5.7	6.5
OC	29.5	31.0	31.0	29.5
PRPE	28.0	16.8	\	30.6
SO2	128.2	123.7	123.7	130.0
TOLU	8.5	7.8	\	8.5
XYLE	7.8	7.5	\	7.8

[a] Results from the standard version of GEOS-Chem v13.3.1 with aircraft emissions excluded (Wang et al., 2022). [b] Total NO emissions including lightning NO. All values are averaged over 2012-2014 in Tg yr^{-1}.

Table S2. Meteorological variables needed for GEOS-Chem v14.0.1.

NO.	Variables	Description	Usage	Unit
		2-D variables		
1	ALBD	Surface albedo	Dry deposition	1
2	CLDFRC	Cloud fraction	Photolysis	1
3	EFLUX	Latent heat flux	Diagnostics	W m^{-2}
4	FRSEAICE	Fraction of sea ice	Hg simulation	1
5	GWETROOT	Root soil wetness	Diagnostics	1
6	GWETTOP	Top soil moisture	CH_4 simulation	1
7	HFLUX	Sensible heat from turbulence	Dry deposition	W m^{-2}
8	FRLAND FROCEAN FRLAKE FRLANDIC FRSNO	Fraction of land/ocean/surface/snow/lake/land ice type in grid box	Chemistry	1
9	LAI	Leaf area index	Diagnostics	m^2 m^{-2}

10	PBLH	Planetary boundary layer height	PBL mixing	m
11	PRECCON	Convective precipitation	Wet deposition	mm day^{-1}
12	PRECTOT	Total precipitation	Wet deposition	mm day^{-1}
13	PARDR	Direct photosynthetically active radiation	Biogenic emissions	W m^{-2}
14	PARDF	Diffuse photosynthetically active radiation	Biogenic emissions	W m^{-2}
15	PHIS	Surface geopotential height	Diagnostics	m^2s^{-2}
16	TROPP	temperature based tropopause pressure	Grid setting	hPa
17	TS	Surface temperature	Chemistry,	K
	TSKIN	Surface skin temperature	deposition Sea salt emissions	K
18	TAUCLI	Optical depth of ice clouds	Diagnostics	1
19	TAUCLW	Optical depth of water clouds	Diagnostics	1
20	SUNCOS	Zenith angle	Chemistry	1
21	SNODP	Snow deposition	Diagnostics	m
22	SNOMAS	Snow mass	Dry deposition	kg m^{-2}
23	SWGDN	Surface incident radiation	Soil NOx; dry deposition	W m^{-2}
24	U10M	10m east-west wind speed	Dry deposition	m s^{-1}
25	USTAR	Friction velocity	Dry deposition	m s^{-1}
26	UVALBEDO	UV albedo	photochemistry	1
27	TO3	Total overhead O_3 column	Photolysis	DU
28	V10M	10m south-north wind speed	Dry deposition	m s^{-1}
29	Z0	Roughness length	Dry deposition	m
30	AREA_m^2	Grid box surface area	Many locations	m^2
31	XLAI	Leaf Area Index	Dry deposition	1
32	LANDTYPEFRAC	Olson fraction per land type	Dry deposition	1
		3-D variables on level edge		
33	PFILSAN	3-D flux of ice non-convective precipitation	Wet deposition	kg m^{-2} s^{-1}
34	PFICU	3d flux of ice convective precipitation	Wet deposition	kg m^{-2} s^{-1}
35	PFLLSAN	3-D flux of liquid non-convective precipitation	Wet deposition	kg m^{-2} s^{-1}
36	PFLCU	3d flux of liquid convective precipitation	Wet deposition	kg m^{-2} s^{-1}
37	CMFMC	Upward moist convective mass flux	Cloud convection	kg m^{-2} s^{-1}
38	PEDGE	Pressure edge for each grid	Grid setting	hPa
		3-D variables on level center		
39	CLDF	3-D cloud fraction	Chemistry	1
40	DTRAIN	Detrainment cloud mass flux	Cloud convection	kg m^{-2} s^{-1}
41	DQRLSAN	Large-scale rainwater source	Wet deposition	kg kg^{-1} s^{-1}
42	DQRCU	Convective rainwater source	Cloud convection	kg kg^{-1} s^{-1}
43	QI	Cloud ice water mixing ratio	Chemistry	kg kg^{-1}

44	QL	Cloud liquid water mixing ratio - anvils	Aerosol microphysics Chemistry	kg kg^{-1}
45	RH	Relative humidity	Aerosol microphysics Many locations	1
46	SPHU	Specific chemistry	Chemistry	kg kg^{-1}
47	T	Temperature	Chemistry	K
48	U	East-west component of wind	Advection	m s^{-1}
49	V	North-south component of wind	Advection	m s^{-1}
50	OMEGA	Updraft velocity	Diagnostics	Pa s^{-1}
51	REEVAPLS	Evaporation of precipitating LS & anvil condensate	Wet deposition	kg kg^{-1} s^{-1}
52	REEVAPN	Evaporation of precipitating convection condensate	Wet deposition	kg kg^{-1} s^{-1}
53	OPTD	Cloud optical depth	Photolysis	1

25

Table S3. Observations and reanalysis data used for model evaluation

Variables	Observation or reanalysis	Data sources or reference
Ozone	WOUDC network	http://woudc.org/data.php (last access: 1 Apr 2025)
	National monitoring networks	Wang et al. (2024)
	OMI satellite (Level 2)	Liu et al. (2010)
	OMI gridded total column ozone	https://disc.gsfc.nasa.gov/datasets/OMTO3d_003/summary (last access: 1 Apr 2025); Ziemke et al. (2017)
NO_2	OMI satellite (Level 3)	https://disc.gsfc.nasa.gov/datasets/OMNO2d_003/summary (last access: 1 Apr 2025); Lamsal et al. (2021)
CH_2O	OMI satellite (Level 3)	https://h2co.aeronomie.be/ (last access: 1 Apr 2025); De Smedt et al. (2015)
CO	MOPITT satellite (Level 3)	https://terra.nasa.gov/data/mopitt-data (last access: 1 Apr 2025); Deeter et al. (2021)
$PM_{2.5}$	Satellite-derived $PM_{2.5}$	https://sites.wustl.edu/acag/datasets/surface-pm2-5/#TOOLS (last access: 1 Apr 2025); Shen et al. (2024)
SWDOWN OLR SWCRF LWCRF	CERES	https://ceres.larc.nasa.gov/data/ (last access: 1 Apr 2025); Kato et al. (2018)
Total precipitation	GPCP	https://psl.noaa.gov/data/gridded/data.gpcp.html (last access: 1 Apr 2025);

		Huffman et al. (2001)
TS Cloud fraction Cloud liquid water	MERRA-2	https://disc.gsfc.nasa.gov/datasets?keywords=MERRA-2&page=1 (last access: 1 Apr 2025)

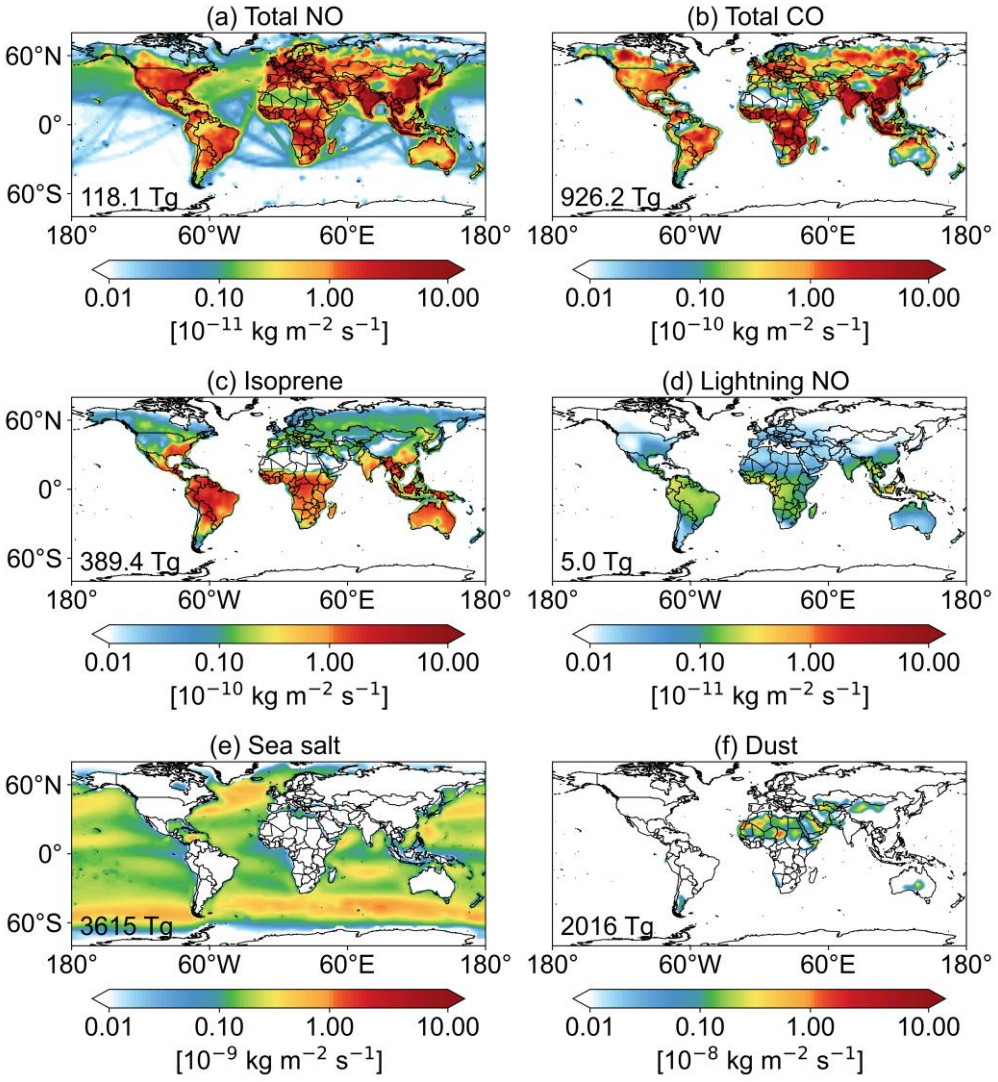

Figure S1. Spatial distributions of annual total emissions used in the study compared to Figure2 in Lu et al. (2020): (a) total NO emissions, (b) total CO emissions, (c) biogenic isoprene emissions, (d) lightning NO emissions, (e) sea salt emissions, and (f) mineral dust emissions. Values are averaged over 2012-2014.

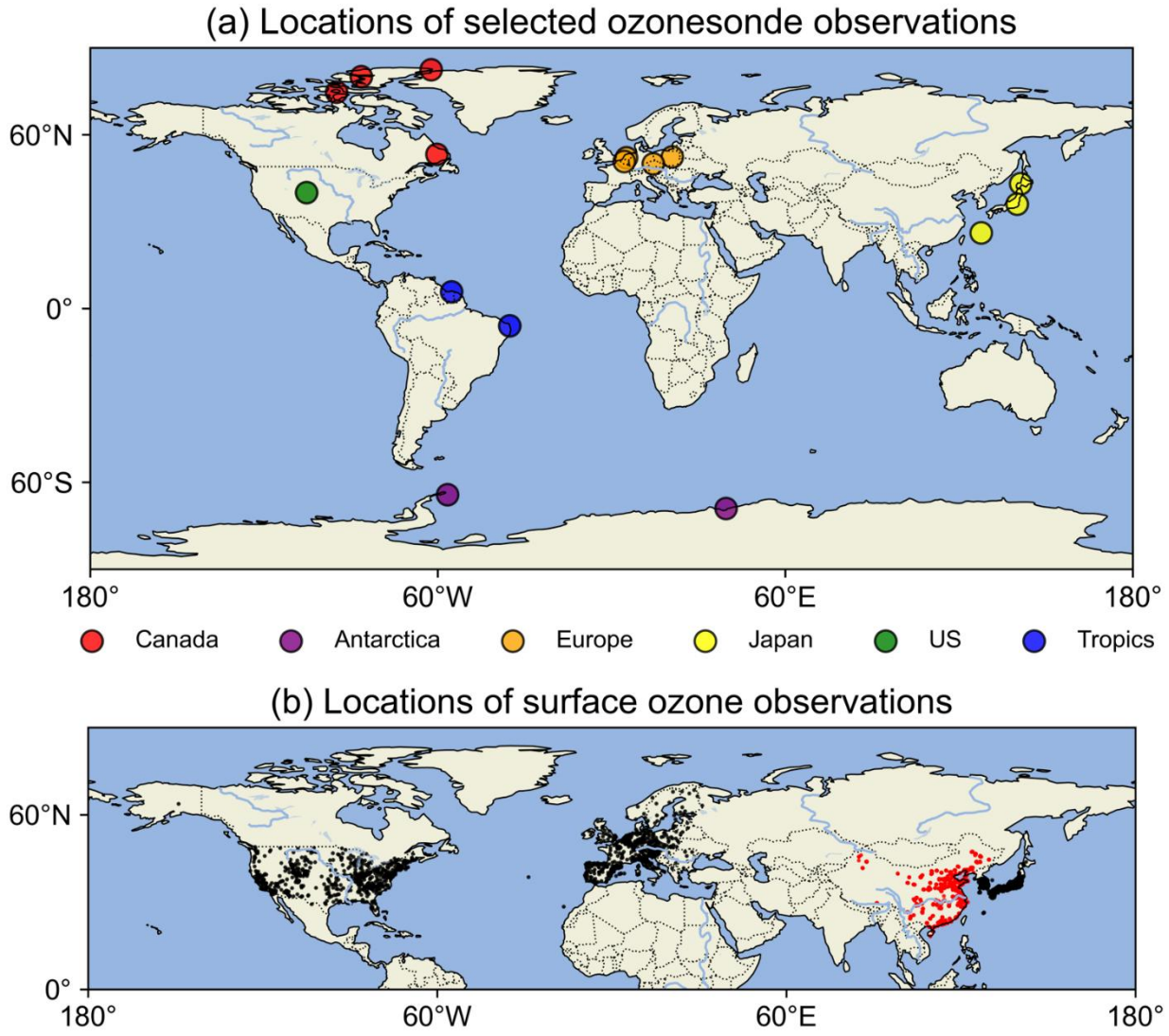

35 **Figure S2. Locations of (a) selected ozonesonde observations, and (b) surface ozone observations used in this study. The black dots in panel b represent rural sites, which are used to evaluate surface ozone at T42L26 simulation, as we do not expect a coarse resolution simulation can resolve urban air pollution. The red dots represent observation sites in China used in Figure 10f. These sites are mostly located at urban or suburban regions.**

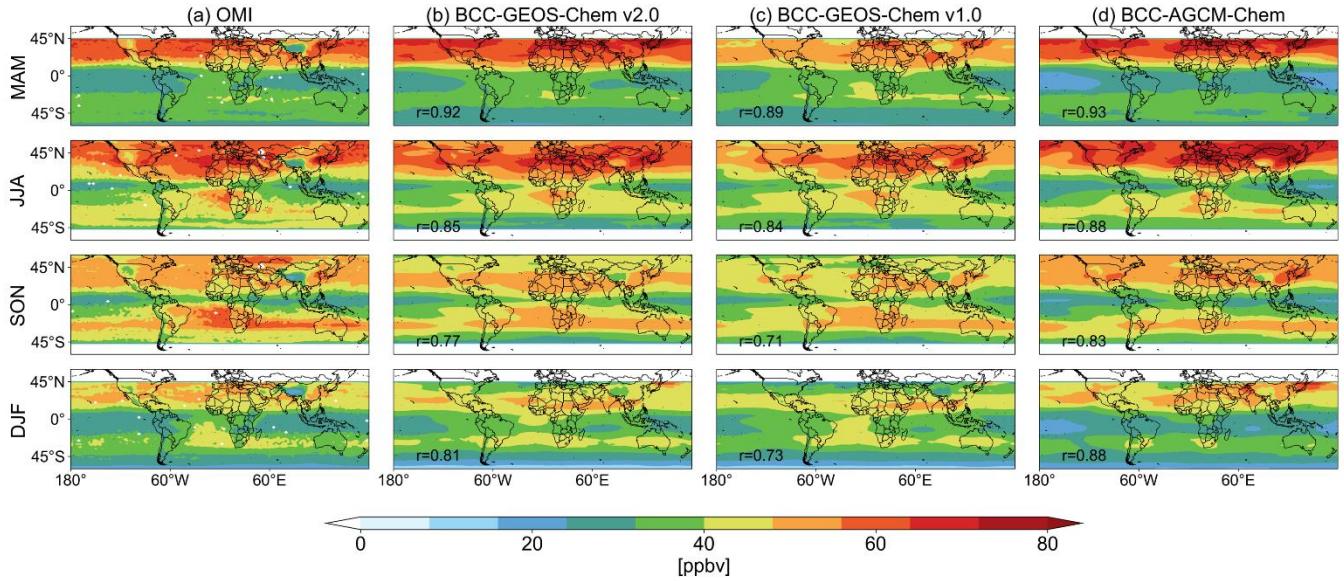

Figure S3. Spatial and seasonal distributions of global mid-tropospheric ozone averaged for 700-400hPa over 2012–2014 from (a) OMI satellite observation, (b) BCC-GEOS-Chem v2.0, (c) BCC-GEOS-Chem v1.0, and (d) BCC-AGCM-Chem. All model outputs are applied with OMI averaging kernels for a proper comparison with the observations.

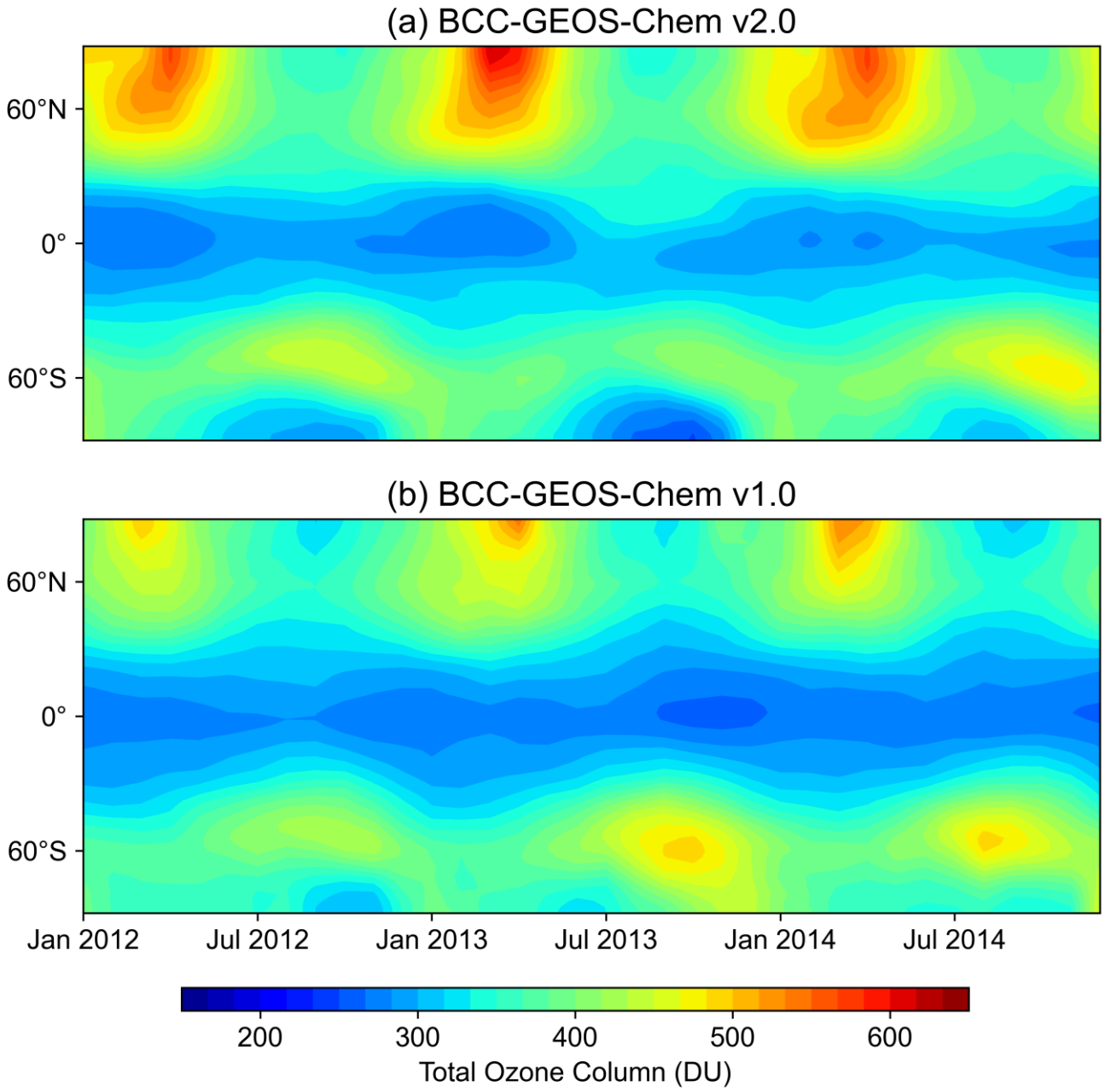

Figure S4. Zonal-mean column ozone over 2012-2014 from (a) BCC-GEOS-Chem v2.0, and (b) BCC-GEOS-Chem v1.0.